Forces in Mechanics 12 (2023) 100208

Contents lists available at ScienceDirect

Forces in Mechanics

journal homepage: www.sciencedirect.com/journal/forces-in-mechanics

Numerical and experimental analysis of sand blasting on polymeric substrates

Erencan Oranli, Nahsan Gungoren, Asghar Heydari Astaraee, Erfan Maleki, Sara Bagherifard *, Mario Guagliano

Politecnico di Milano, Via G. La Masa 1, 20156, Milan, Italy

ARTICLE INFO

Keywords:
Polymers
Surface treatment
Sand blasting
Finite element analysis

ABSTRACT

In view of the recent interest in modifying the surface functionality and esthetics of polymeric materials by sand blasting treatment, a numerical model was developed as a tool to predict the evolution of surface morphology as a function of blasting parameters. The wide range of shot size and shape variations, typical of blasting media, were parametrized based on microscopical observations. Thus, the developed numerical model accounts for the media inhomogeneity and also implements randomness in both the sequence and position of the multiple impacts. To make the model as realistic as possible, the velocity of individual shots was calculated based on their interaction with the airflow. Systematic experiments were performed using Polycarbonate (PC) as the substrate material and Alumina as the blasting media. A comparison of the experimental and numerical results demonstrated the ability of the developed model to successfully predict the surface roughness generated by sand blasting, as the shot arrangement and distribution were varied. This model establishes a potential basis for future studies regarding the performance of the sand blasted surfaces such as wettability using numerical approaches.

1. Introduction

In the last decade, surface patterning and modifying the surface morphology have attracted considerable attention due to their beneficial effects on providing components with hydrophilic/hydrophobic surfaces, high biocompatibility, bactericidal properties, etc. [1]. Sand blasting is a promising treatment for modulating the surface properties of polymeric materials. The possibility of reusing and recycling the impacting media during a series of sand blasting processes makes it cost-efficient and scalable. The main motivations behind the application of sand blasting have been to remove contaminants or oxide scales from metallic surfaces. It has also been used prior to painting to enhance surface area and gripping. The effect of sandblasting on the surface properties of steel has been studied under pressures of 1,2 and 4 bar [2]. Surface roughness was one of the main properties that were under examination in this study since sand blasting has also a high potential to modulate the surface roughness. Roughness is a characteristic that affects many interaction-related features of a material and its performance under different types of loading. Thus, the ability to control it can bring in new opportunities and applications for the material.

The technical prospect of sand blasting is quite similar to shot peening. The current technology of shot peening ensures a fine control of the shot morphology, shot size, impact velocity, air flow pressure, and stand-off distance. In both treatments, accelerated shots impact the substrate surface and create dimples as a result of plastic deformation. In shot peening applications, the main motivation is to enhance the life of a component under fatigue loads by inducing plastic deformation and surface compressive residual stresses. Even if plastic deformation takes place with the same functionality, sand blasting has been mainly used to prepare the surface for the following process. From the material point of view, shot peening is mainly applied to metallic materials. However, in sand blasting applications, different material families can also be used thanks to the lower kinetic energy of the process.

The main parameters of sand blasting besides media characteristics are air pressure, stand-off distance (SoD), and blasting time. The resulting surface morphology strongly depends on the substrate and shot properties. As the plastic deformation will be induced by the kinetic energy of the impacting media, the impact velocity is a key factor. It is highly influenced by air pressure and SoD as well as the shot shape, size, and material.

Contrary to the highly controlled shots used in shot peening treatment, in sand blasting, the media used to impact the substrate can be of

* Corresponding author.
E-mail address: sara.bagherifard@polimi.it (S. Bagherifard).

https://doi.org/10.1016/j.finmec.2023.100208
Received 10 February 2023; Received in revised form 25 May 2023; Accepted 2 June 2023
Available online 3 June 2023

various types including sand, shot (in metal applications), glass, coconut shells, and even dry ice, with fewer restrictions on the size distribution and shape consistency. Soft blasting, referred to also as soda blasting, which is another special application with a similar approach (using blasting media of sodium-bicarbonate ($NaHCO_3$)) was applied on Polytetrafluoroethylene (PTFE), commercially known as Teflon samples in a study by Menga et al. [3] where superhydrophobic surfaces were efficiently obtained after a few seconds of the treatment.

Sand blasting on metallic components as a preparation treatment for posterior applications has already been the topic of several researches. For example, Melentiev et al. [4] utilized white aluminum oxide as media to perform a micro-blasting operation on bio-medical Co-Cr-Mo alloy. Raykowski et al. [5] examined the effect of sand blasting using two types of media as stainless steel and spherical glass to clean the gas turbine components; these included compressor blades made of AISI 403 stainless steel and discs made of ASTM A294 Class 5 steel alloy and covered with aluminum coating for protection. Chintapalli et al. [6] utilized sand blasting in the dental restoration sector. Chintapalli et al. [7] used sand blasting to treat 3Y-TZP to examine the effect of different blasting conditions such as different shot size, air pressures, and impacting angles on the mechanical properties of the substrate.

The application of sand blasting on polymers has been also investigated in various research studies. Rocha et al. [8] applied sand blasting on a PEEK substrate, which was stated to be a viable candidate material for dental prostheses, using 45 μm particles of Aluminum oxide for an exposure time of 15 s. The blasting pressure and SoD were 2.8 bar and 10 mm, respectively. Results showed that after the treatment, better adhesion among PEEK, resin cement and dentin was observed. Ourahmoune et al. [9] applied sand blasting on six different PEEK materials consisting of two unreinforced grades and four reinforced composites. The aim of the study was mentioned as providing a correlation between the process parameters of sand blasting and wettability through contact angle measurements. Blasting pressure was set to 5 bar and the SoD was 80 mm whereas exposure time and blasting media size were varied. The range for the exposure time was from 5 to 30 s and the average particle sizes for Aluminum oxide media were 50, 110 and 250 μm. It was concluded that sand blasting altered the hydrophobicity of the material for all six different grades by modifying the surface morphology. In another research done by Porrelli et al. [10], sand blasting of PEEK using Aluminum oxide particles with a particle size of 125 μm was studied where the substrate was mentioned as a suitable alternative for replacing titanium implants regarding its stability and similar mechanical properties to the bone tissue. While the SoD and exposure time were varied, the pressure was fixed at around 3 bar. It was found that sand blasting was efficient in increasing the roughness and wettability of PEEK. Lampin et al. [11] investigated the effect of different roughness levels of PMMA obtained by sand blasting with different sizes of Aluminum oxide particles (50–125–250 μm). The pressure was also varied between 2 and 4 bar while exposure time was set at 10 s. An increased roughness achieved by sand blasting enhanced the cell adhesion. Recently, Chen et al. [12] examined the effect of induced roughness on the cold spray deposition efficiency of ABS and PEEK substrates for the tin coating. Besides using direct grit blasting, an indirect way of applying grit blasting over hot pressing was also investigated in the study. It was concluded that an induced roughness on the surface of the polymeric substrate positively affected the coating thickness but had a negative effect on its adhesion strength.

In view of optimizing the sand blasting treatment with respect to its objective, the development of a numerical model able to accurately assess the final result of the treatment as a function of the process parameters is of great interest and would considerably reduce the effort for the experimental tuning of sand blasting.

Yu et al. [13] proposed a numerical model for sand blasting on wind turbine blades. It was stated that sand blasting was seen as a replacement for manual grinding of the blades and the comparison of the two treatments was to be done over the durability of the posterior painting on the blade surface. The model was demonstrated as a fluid dynamics one with the outcomes both in the fluid flow and the structural domains (such as the numerical roughness data). However, no details regarding the structural modeling were provided. In the study by Gerhardter et al. [14], a series of simulations were done through a 2D axisymmetric model using ANSYS Fluent for comparing two different types of sand blasting nozzles. The evaluation was performed over the particle velocity at different SoDs. Having the motivation regarding the effectiveness of nozzle geometry, the model only provided insights for fluid dynamics modeling.

Despite the increasing interest in sand blasting of polymers, there are no studies, to the best of the authors' knowledge, on the structural modeling of sand blasting on polymeric materials. Even the study by Yu et al. [13] does not propose any clear structural modeling of the treatment. Furthermore, they used spherical solids for representing the abrasive particles which is not usually a representative case for sand blasting with non-spherical media.

It is of great importance to highlight the effects that can bring the surface treatment of polymers using sand blasting to tailor their surface morphology. A numerical finite element (FE) model of the blasting in this regard not only would relax the experimental effort and cost but also would create an interface for future studies where process parameters, surface roughness and properties can be related through machine learning algorithms.

Considering the common concepts between sand blasting and shot peening, we reviewed the numerical models of shot peening widely developed in several scientific studies. These studies focused on different parameters including the effects of process parameters on the final surface state through numerical models, including the effect of randomly located shot impacts rather than referring to *a priori* arrangement [15], peening simulation of Almen strip in FE domain to relate Almen intensity and residual stresses [16], analyzing the effect of shot size using a wide range of media [17], the effect of different constitutive material models for the substrate and how it affects residual stress and roughness [18], the effect of shot peening time, coverage rate and impact velocity on residual stress state and surface roughness in high manganese steel [19], and the influence of coverage on residual stress state and surface roughness of carburized roller made of 18CrNiMo7–6 steel [20]. Multiple impact numerical model of shot peening and similar treatments have also been developed in our research group for analyzing the evolution of main surface roughness parameters [21], quantitative surface coverage assessment [22], prediction of grain refinement in the surface layer after severe shot peening (SSP) [23], and utilization of numerical model to estimate the final surface morphology of laser powder bed fusion AlSi10Mg samples after shot peening [24]. It is noted that the last study initialized the numerical model of shot peening from the as-built state, thus accounting for the initial state of surface morphology through surface digitalization.

In this study, we introduce a numerical approach based on our previous shot peening models [21–23] to simulate the sand blasting process considering the variety in the shape and size of the blasting media. As this variety was expected to influence the impact velocity of the shots, a consecutive study was followed to assess the impact velocity of individual shots as a function of their size and morphology. Dimple size and mesh convergence analyses were performed, and eventually, data post-processing was applied to evaluate the surface roughness parameters and their variation as a function of blasting parameters. Sand blasting experiments were performed in parallel to find the optimum working conditions of the equipment, followed by the roughness measurement on the treated samples. Comparing the surface roughness data obtained from the experimental and numerical analyses, validated the efficiency of the developed model for assessing the evolution of surface roughness developed on polymeric substrates by sand blasting.

2. Experimental procedure

2.1. Material

Polycarbonate (PC) was selected as the substrate material due to its relatively low cost, high stiffness and ultimate tensile strength, and its availability among other thermoplastic polymers. It is noted that for the purpose of the current study, thermoplastic polymers are the best option due to their ability to be deformed plastically without considerable damage at room temperature. A flat PC sheet was cut into 50 × 50 × 5 mm^3 samples. An adjustable set-up stand was developed to control the SoD between the nozzle and the substrate. As the blasting media, Alumina was chosen due to its relatively high hardness with excellent recyclability and cost-effectiveness properties and its wide application in sand blasting of polymers [8–11].

2.2. Sand blasting

A Guyson Formula F1600 blasting machine was used for the experiments. Preliminary tests indicated that the machine performance was stable considering 3 s of operation and a minimum air pressure of 6 bar. Fixing these parameters, multiple sets of sand blasting experiments were performed with varying SoD (100 mm, 150 mm, and 200 mm) to identify the optimum SoD for experimental studies. Before SoD selection, a coverage assessment procedure was set. Coverage was defined as the ratio of the plastically deformed area over the total area and determined through visual inspections by scanning electron microscopy (SEM) [25].

2.3. Roughness measurement

Surface roughness measurements were performed using a Mahr PGK Perthometer with a probe tip radius of 2 μm, following ISO 4288 instructions. According to the standard, a cut-off wavelength equal to 0.25 mm was selected, to distinguish the shorter and longer wavelengths in the profile signal (roughness vs. waviness profiles). Correspondingly, the evaluation length was selected to be 1.25 mm where the total movement length of the probe was 1.75 mm. Considering the aperiodic behavior of the sand blasting process and the high irregularity of the impacting media's shape and size, 3 samples were prepared for each set of blasting parameters to evaluate the repeatability of the results. 7 measurements were performed on each sample and thus 21 measurements were obtained in total per parameters set. Fig. S1 shows the schematic illustration of the surface roughness measurement phase. The list of standard roughness parameters evaluated in this study and their definition is provided in Table 1 where the Z function indicates the filtered roughness data and L refers to the evaluation length. To better explain R_z and R_{max}, sampling length concept must be highlighted. The evaluation length was segmented into 5 pieces each having a length of 0.25 mm. In each of these segments, a local R_t (R_{ti}) was evaluated. R_z was calculated as the average of these 5 values, whereas R_{max} is their maximum value.

Table 1
Standard line profile roughness parameters according to ISO 4288 standard [26].

Parameter notation	Description	Formula
Ra	Arithmetical mean of absolute values of entire roughness data over evaluation length	$= \frac{1}{L}\sum_{i=1}^{L}\lvert Z_i\rvert$
Rq	Root mean square of entire roughness data over evaluation length	$= \sqrt{\frac{1}{L}\sum_{i=1}^{L} {Z_i}^2}$
Rt	The difference between the highest peak and lowest valley of the roughness profile over evaluation length	$= \max(Z) - \min(Z)$
Rz	The average of 5 peak-valley distances over evaluation length	$= \frac{1}{5}\sum_{i=1}^{5} R_{ti}$
Rmax	Maximum of the 5 peak-valley distances over evaluation length	$= \max(R_{ti})$

3. Numerical simulation

3.1. Material model

Material properties of the substrate are provided in Table 2. To consider the plastic deformation behavior of the substrate in the simulation, the rate-dependent Johnson-Cook material model was utilized, since it is able to account for relatively high strain rates ($10^6\ s^{-1}$) emanating from the high velocity of blasting media during sand blasting. It is noted that for the blasting process with repeated impacts, not only the strain rate effects but also the cyclic behavior of the material can play a role. This requires a more sophisticated material model with combined kinematic-isotropic hardening which was beyond the scope of the current study. Further analysis on the accuracy of the material model will be considered as future work. As regards the blasting media, Granta EduPack 2021 R2 [27] was used as the material reference database. The properties of Alumina were taken as the mean value of the given range, as shown in Table 2.

3.2. Sample and media characterization

To better examine the surface coverage induced by sand blasting, images of treated specimens were captured using Zeiss Evo 50 SEM. The substrate was coated with gold to render the maximum resolution.

Characterization of the media shape and size was also accomplished by analyzing SEM images of the media particles. A total of 210 particles were analyzed. A representative image from the SEM image set of Alumina media is shown in Fig. 1a. Based on the visual examination, four main categories of the shot shape were defined as spherical, ellipsoidal, cuboid, and tetrahedron; these will be referred to as "groups" hereafter. Although this grouping is not fully inclusive, it is an effective approach to parametrize the wide shape variation to enable the development of the numerical model. The shot geometries produced by Catia V5 R19 are shown in Fig. 1b. The size of the shots was categorized (hereafter called "sub-groups") by considering the cross-sectional areal data obtained through image analysis using ImageJ 1.52a software. The sub-groups were defined as the 1/3rd and 2/3rd thresholds of the cross-sectional area ranges by evaluating the difference between max and min areas measured in SEM images for each group; accordingly, these were labeled as "small", "medium", and "large", leading to a total of 12 shot sub-groups to define size and morphology of the media. The number of particles and their distribution in each sub-group is shown in Fig. 1c while the relevant number fraction is shown in Fig. 1d. These fractions were used as the weighting coefficients when producing random shot positions in the multiple-impact sand blasting model (section 3.4.3). A MATLAB code was developed to group the particles into corresponding sub-groups by considering their sizes and deriving the required dimensional information for each shot.

3.3. Shot velocity evaluation

Evaluation of shot velocity is critical for developing an efficient numerical model as it determines the impact energy and thus, the extent of the induced deformations. A model developed by Kirk [29] was used to estimate peening shot velocity by accounting for the contribution of the shot's density and size, as well as nozzle dimensions while taking the air acceleration constant inside the nozzle. Another methodology developed by Li et al. [30] quantified the shot velocity in abrasive jet micromachining (AJM) by considering two main segments i.e., inside the nozzle length and after the nozzle to consider different acceleration phases. They calculated the shot velocity at the end of the phases considering a constant shot acceleration within each one. Liu et al. [31] further updated the model mainly stating that once the air-shot stream leaves the nozzle and starts its path through SoD, the air density will

Table 2
Material properties of PC [28] and Alumina (90 wt%) [27] used in the FE model.

Material	Young's modulus (GPa)	Poisson ratio	Density (kg/m^3)	A (MPa)	B (MPa)	n	m	C	$\dot{\varepsilon}_0$
PC	2.59	0.39	1200	80	75	2	0.548	0.052	0.005
Alumina	286	0.215	3525	–	–	–	–	–	–

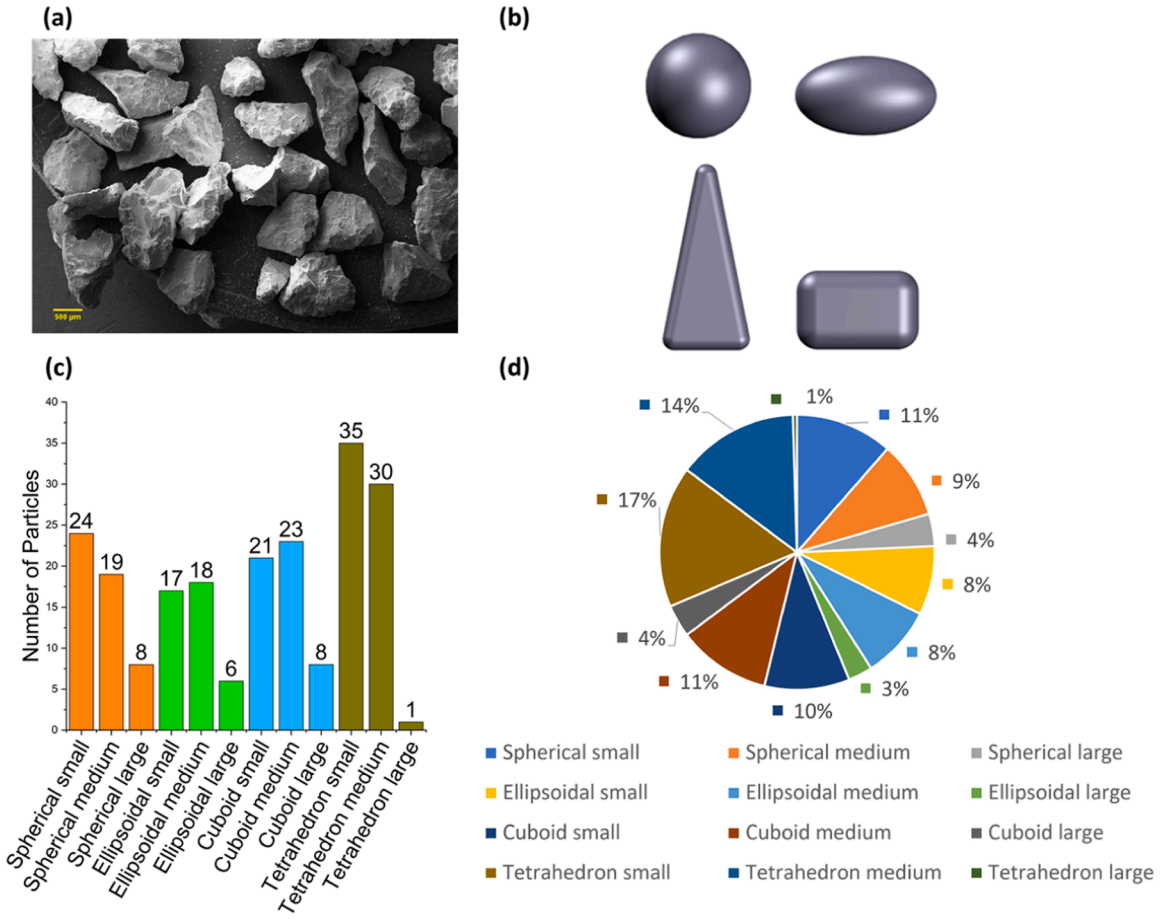

Fig. 1. a) A representative SEM image of Alumina blasting media b) 3D illustration of morphological groups considered for the media c) histogram of sub-groups d) pie chart of sub-groups.

Table 3
Nozzle, air stream, and shot parameters used for shot velocity evaluation.

Parameter	Value
Length of the nozzle (l_n)	65 mm
Diameter of the nozzle (d_n)	8 mm
Density of shot material (ρ_s)	$3525 \frac{kg}{m^3}$
Air pressure (p)	4 – 6 bar
Temperature (T)	298.15 K
Length of a single segment, inside and after the nozzle (l_s)	0.1 mm
Adiabatic exponent of air (K)	1.4
Ambient air pressure (P_0)	1 atm
Individual gas constant of air (R_i)	287 Nm/kgK
Air density at ambient temperature (ρ_a^0)	$p_0/(R_i \times T)$
Surface area of shot (A_s)	Varying for all shot sub-groups
Mass of shot (m_s)	Varying for all shot sub-groups
Drag coefficient (C_D)	Varying for all shot sub-groups

vary as well. Thus, they proposed a new model based on the segmentation logic suggested in [30] while accounting also for air density variation after the nozzle exit.

A MATLAB routine was developed following the methodology described in [29–31] to evaluate shot velocity considering the irregular shape of the shots, the corresponding variation of the drag coefficient, and also based on the nozzle dimensions of the sand blasting equipment. All the input data are listed in Table 3. The velocity calculation algorithm is presented in Fig. 2a while a representative output of the code is shown in Fig. 2b and c with various air pressures for small spherical and large spherical particles, respectively.

3.4. FE modelling

FE model was built up using ABAQUS/Explicit 2019 Software. The substrate was modeled by a representative 3D cube with the dimensions of 6 × 6 × 3 mm^3, as shown in Fig. 3a. Half-infinite elements were inserted on the side walls and the bottom face to provide quiet boundaries and avoid the reflection of the stress waves back into the model. A

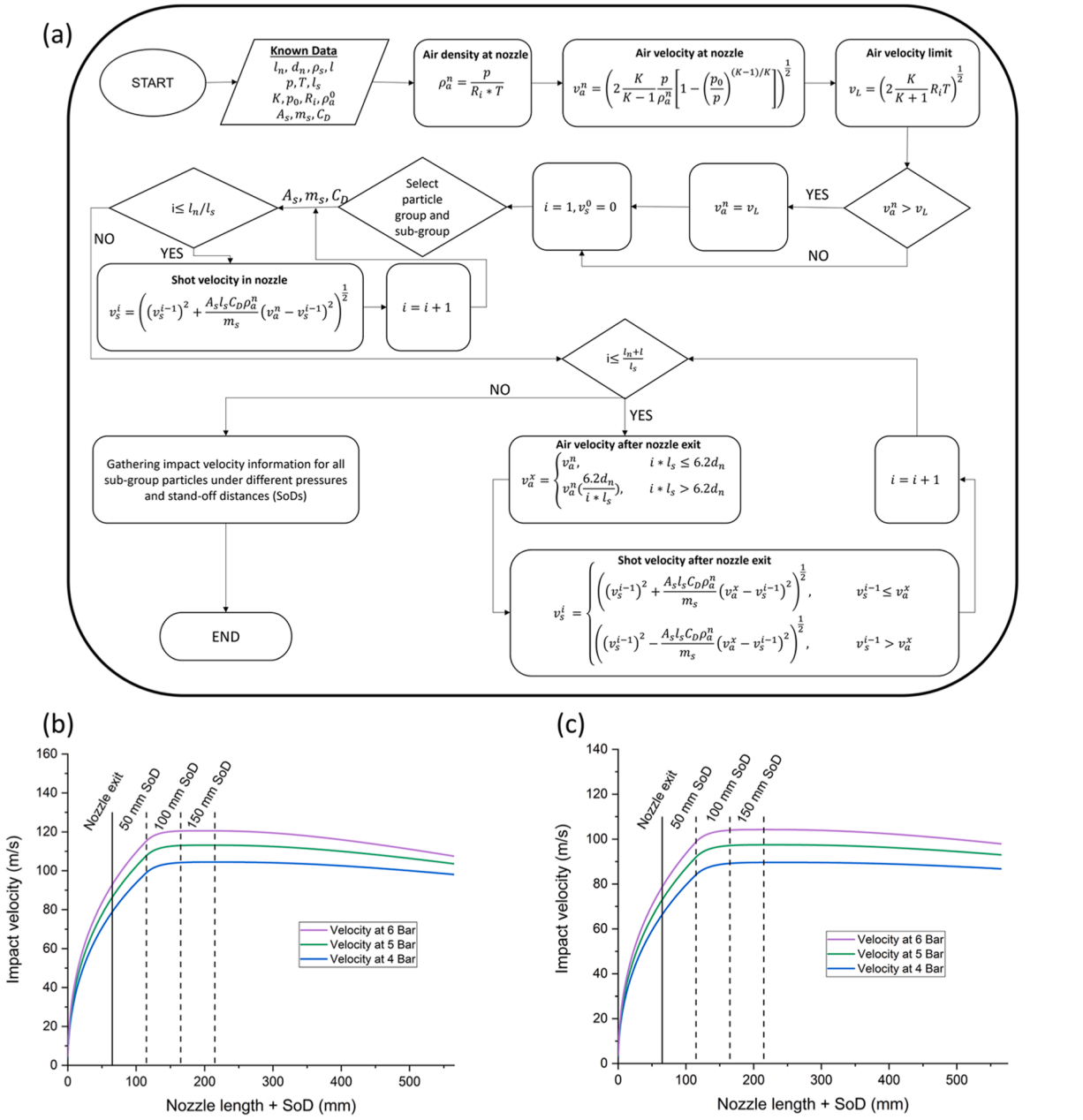

Fig. 2. a) Flowchart describing the algorithm developed for shot velocity evaluation. Variation of shot velocity as a function of distance from shot injection point for b) small spherical shots c) large spherical shots.

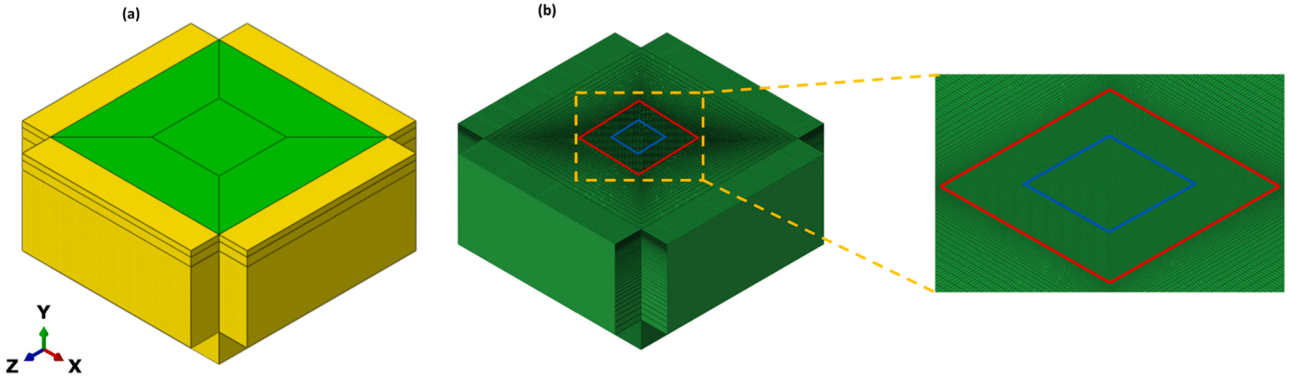

Fig. 3. a) Substrate model geometry b) mesh details of the FE model.

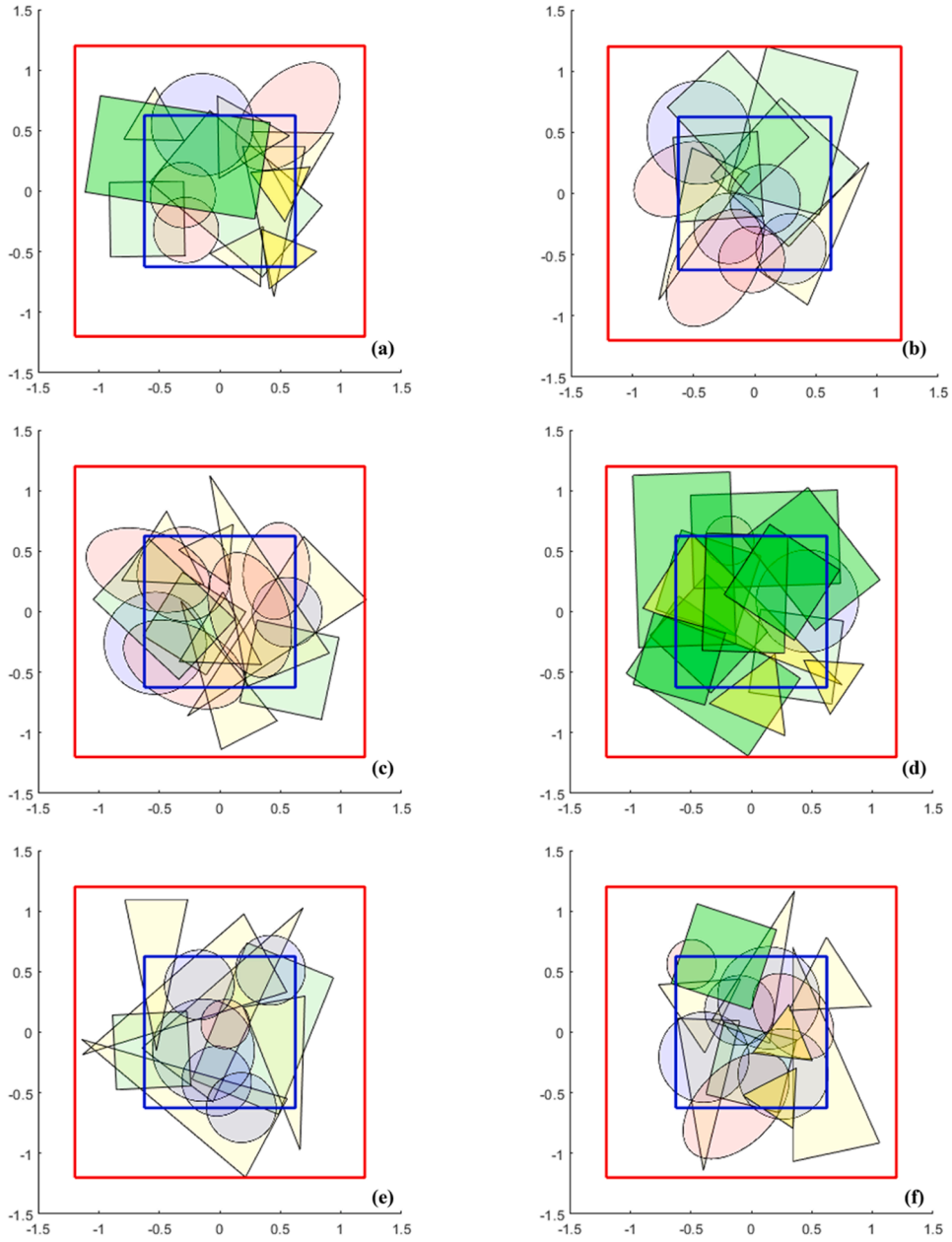

Fig. 4. Random positioning of the shots in the impact area to obtain full coverage (the blue rectangle represents the boundaries of the impact area while the red rectangle defines the area with the refined mesh) for a) set-1 b) set-2 c) set-3 d) set-4 e) set-5 and f) set-6.

face partition was introduced on the upper surface (referred to as the impact area). The required data for modeling the shots were obtained as described in section 3.2. A representative meshed model is shown in Fig. 3b where red rectangle demonstrates the boundaries of the area with refined mesh and the blue rectangle shows the boundaries of impact zone. The substrate was meshed with 1,007,160 elements of C3D8R type (8-node linear brick elements with reduced integration and hourglass control). The model also included 42,460 half-infinite CIN3D8 elements. Mesh convergence studies were performed, and an element size of 0.022 mm was selected for the impact area to make the results independent of the mesh size. The shots were also meshed using C3D8R elements with a dimension of 0.022 mm.

The vertical displacement of surface nodes after a single impact simulation was examined to evaluate the dimensions of the corresponding dimple that is the indentation generated on the surface due to the high-velocity impact of the shot. A regression approach was implemented to estimate the dimple dimensions required for surface coverage. Minitab 20.4 was utilized to perform the regression analysis. Initially, a series of single impact simulations were performed in ABAQUS per each shot group with 3 different impact velocities obtained from the velocity estimation model (section 3.3); these include the minimum, average and maximum velocities obtained with pressure levels of 4, 5 and 6 bar and SoD levels of 50, 100 and 150 mm. The resulting dimple dimensions were put into regression models coupling them with the corresponding shot dimensions and velocities to ensure an efficient model that would give accurate results with intermediate values of input factors of pressure and SoD. The regression models were then used to extract dimple dimensions for selected air pressure and SoD to be used in Eq. (1) for the random position generation in the multiple-impact sand blasting model. The average R^2 value of all the regression models was 97%. This confirmed the validity of the approach to serve as an efficient coverage estimation tool for the multiple-impact sand

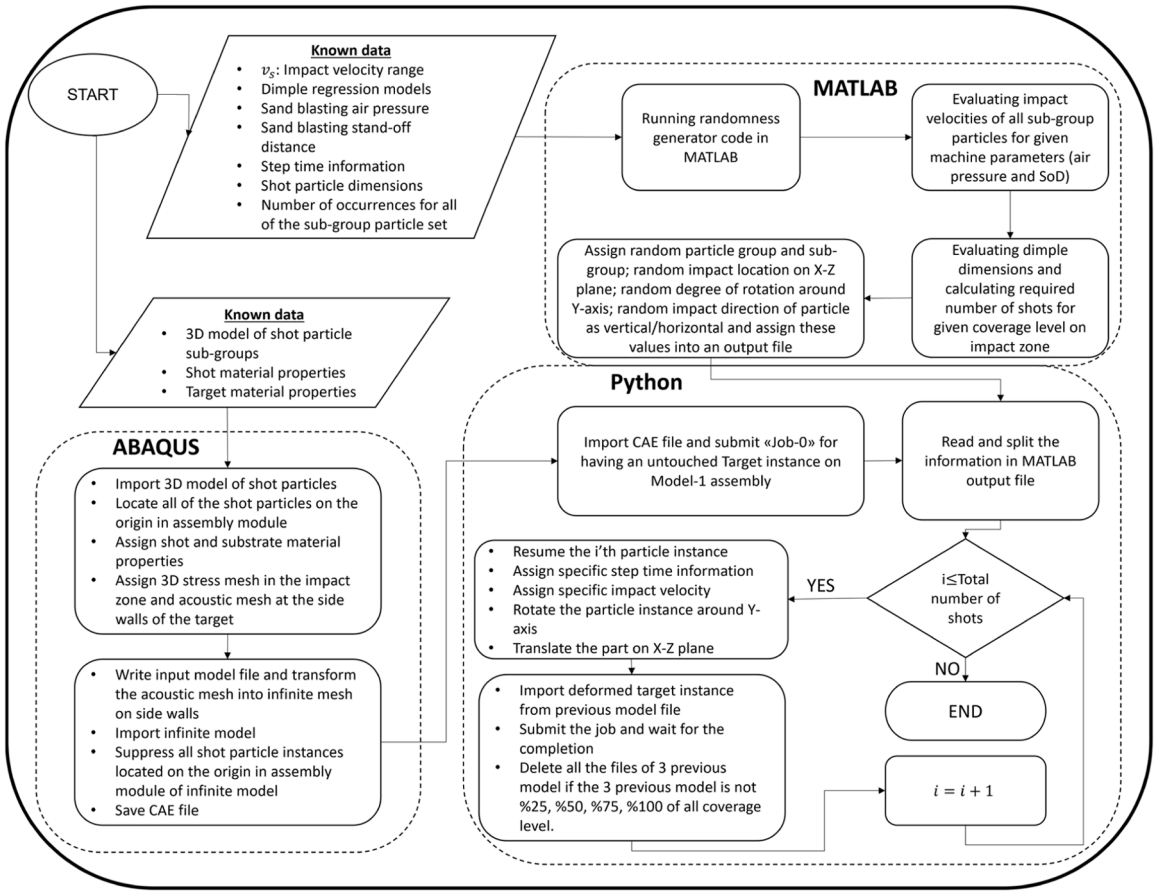

Fig. 5. Algorithm of multiple-impact modeling.

blasting model.

The shape, size, velocity, and orientation of the shot affect the required time for a single-shot impact model. Single impact simulations were developed for all the groups and sub-groups to gather the relevant data regarding the sufficient time required for shot detachment from the surface after impact.

3.4.1. *Multiple-impact modeling*

A MATLAB routine was developed to produce random shot positions required for the multiple-impact sand blasting model. The initial requirement was to evaluate the number of shots needed for a specific coverage level. Highly preferred and used Avrami equation was utilized for this purpose as in the way it was established and used in the studies of Kirk and Abyaneh [32–35] based on the consecutive studies of Avrami [36–38]. Considering the theoretical impossibility of reaching full coverage, 98% coverage level is accepted as the full coverage [39]:

$$Cov\% = 100\left[1 - e^{-Ar}\right] \tag{1}$$

where Ar refers to the ratio of the indented area to the total impact area. The indented area is equal to the multiplication of the shot number with the average dimple area that was evaluated by taking the weighted average of all dimple areas obtained in dimple size regression (section 3.4.1). The total impact area was set to 1.25×1.25 mm^2. Assigning a coverage value ensures the accurate evaluation of shot number as it remains the only unknown in the Avrami equation. Having calculated the required number of shots from Eq. (1), sets of 5 random data were generated as below:

- Random selection of shot group (shape)
- Random selection of shot sub-group (size)
- Random selection of shot orientation (vertical or horizontal) for non-spherical shots
- Random rotation of shot around the Y-axis
- Random translation on the XZ plane

It is noted that full randomization of the particle impact orientation for non-spherical particles was not feasible due to the singularity problems arising from certain impact directions. Thus, two vertical and horizontal orientations were taken into account resulting in different indent shapes. For the horizontal orientations, contact with the substrate has been provided through the larger base for cuboid, one of the side surfaces for tetrahedron, and the larger contact surface for ellipsoidal particles. Whereas on the vertical orientations, smaller base surface contact for cuboid, single base surface contact for tetrahedron and smaller contact surface for ellipsoidal particles has been provided.

In total, 6 random sets of impact sequences are generated as shown in Fig. 4, in which all the above-mentioned aspects are implemented. Having 12 sub-groups at hand and positioning non-spherical shots in two orientations made a total of 21 possible impact situations. A Python routine was developed to manage the multiple-impact simulations running consecutive single-shot impact models by resuming a specific shot in the model and then positioning it randomly over the impact area. For each successive impact, the deformation history of the substrate was imported from the previous analysis. The algorithm of the numerical model including the python script is summarized in Fig. 5.

3.5. *Roughness evaluation*

Surface morphology and roughness parameters were evaluated on the impact zone. Vertical displacement data of the surface nodes were

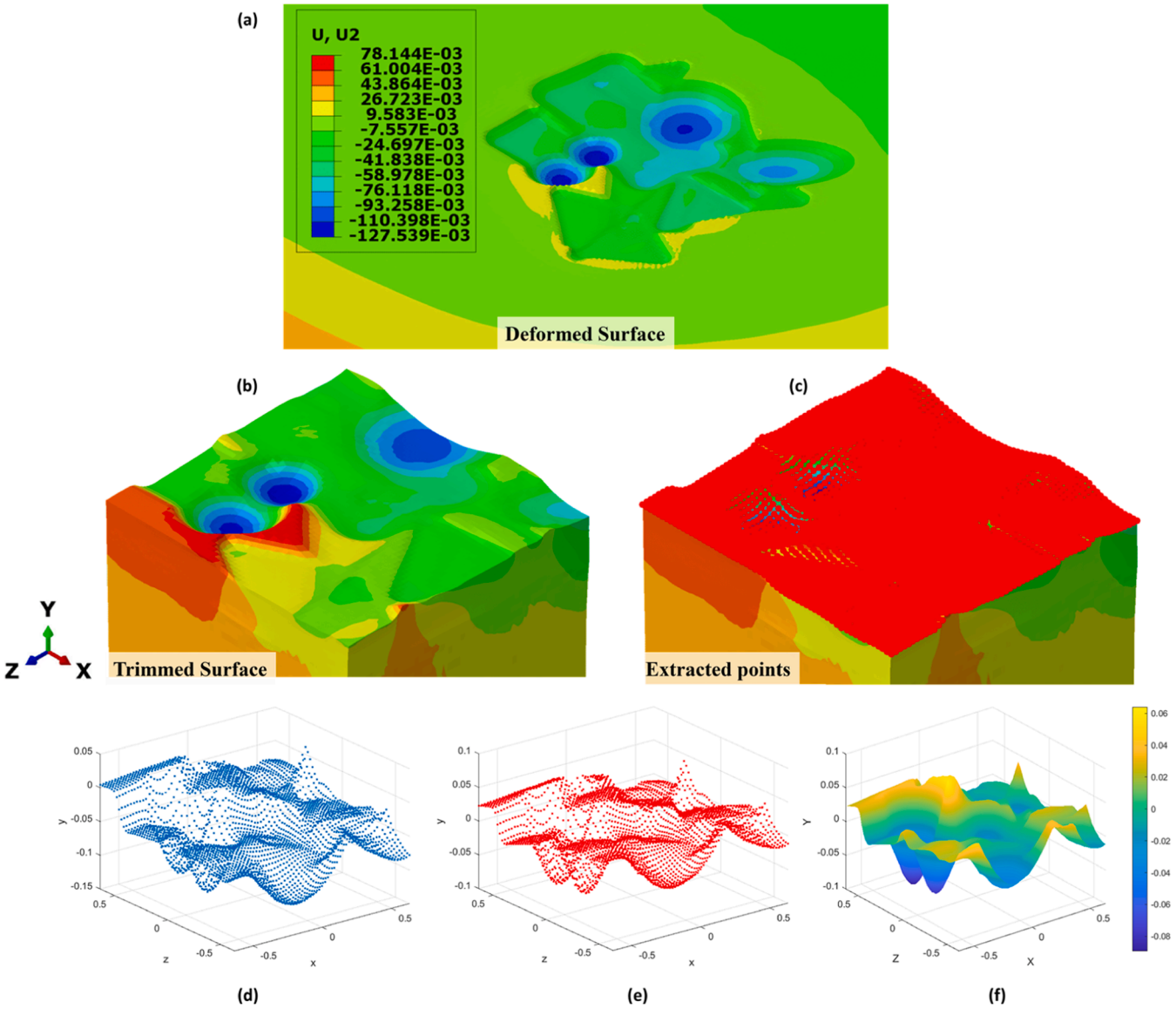

Fig. 6. Representative deformation contour of the surface used for roughness data extraction a) output of the simulation b) trimmed impact surface c) data point extraction; MATLAB processing steps d) original set of coordinates of data points e) filtered surface after removing slope in y-direction f) smoothed data.

extracted for further processing as the primary profile. Fig. 6a, b, and c show the final deformed substrate surface and the phases of data processing to extract the standard roughness parameters. Filtering must take place to extract roughness. A MATLAB routine was developed to separate waviness (low-frequency features of the profile) and roughness (high-frequency features of the profile), considering a cut-off wavelength of 0.25 mm following the methodology proposed by [24]. In brief, the routine receives the original set of nodal coordinates, removes the slope in the y-direction, and smoothens the data for further evaluation (Fig. 6d, e, and f).

4. Results and discussion

4.1. Experimental results

4.1.1. Surface morphology

The effects of the two main process variables, i.e., air pressure and SoD on the induced surface coverage and morphology are investigated in this section. Fig. 7 depicts the surface morphology of the sand blasted PC after 3 s exposure time using different air pressure and SoDs. Fig. 7a and b show the surface morphology for pressures of 4 bar and 6 bar, respectively, with identical SoD and exposure time. More separated indentations are observed for the specimen treated by 4 bar air flow pressure, indicating less homogenized dispersion of the impacts and lower coverage level. The dimples were better dispersed over the impact zone when air flow pressure was increased to 6 bar. A higher pressure seems to have promoted the homogeneity of plastic deformation. However, contrary to the case of 6 bar treatment, the state of the surface did not reach the full coverage level with 4 bar for the same exposure time.

Regarding the effect of SoD on coverage, a preliminary evaluation was done based on the results described in Fig. 2b and c. Impact velocity was found to be independent of SoD in the range of 100 mm to 350 mm. The experiments were performed varying SoD in this range and keeping air flow pressure of 6 bar and exposure time of 3 s. The surface morphologies of blasted PC specimens under these conditions are presented in Fig. 7c and d. These observations confirmed that starting from an SoD of 200 mm, the coverage level decreased. As observed in Fig. 7, the SoD level of 150 mm provided a homogeneous distribution of impacts over the impact zone while maintaining the impact velocity.

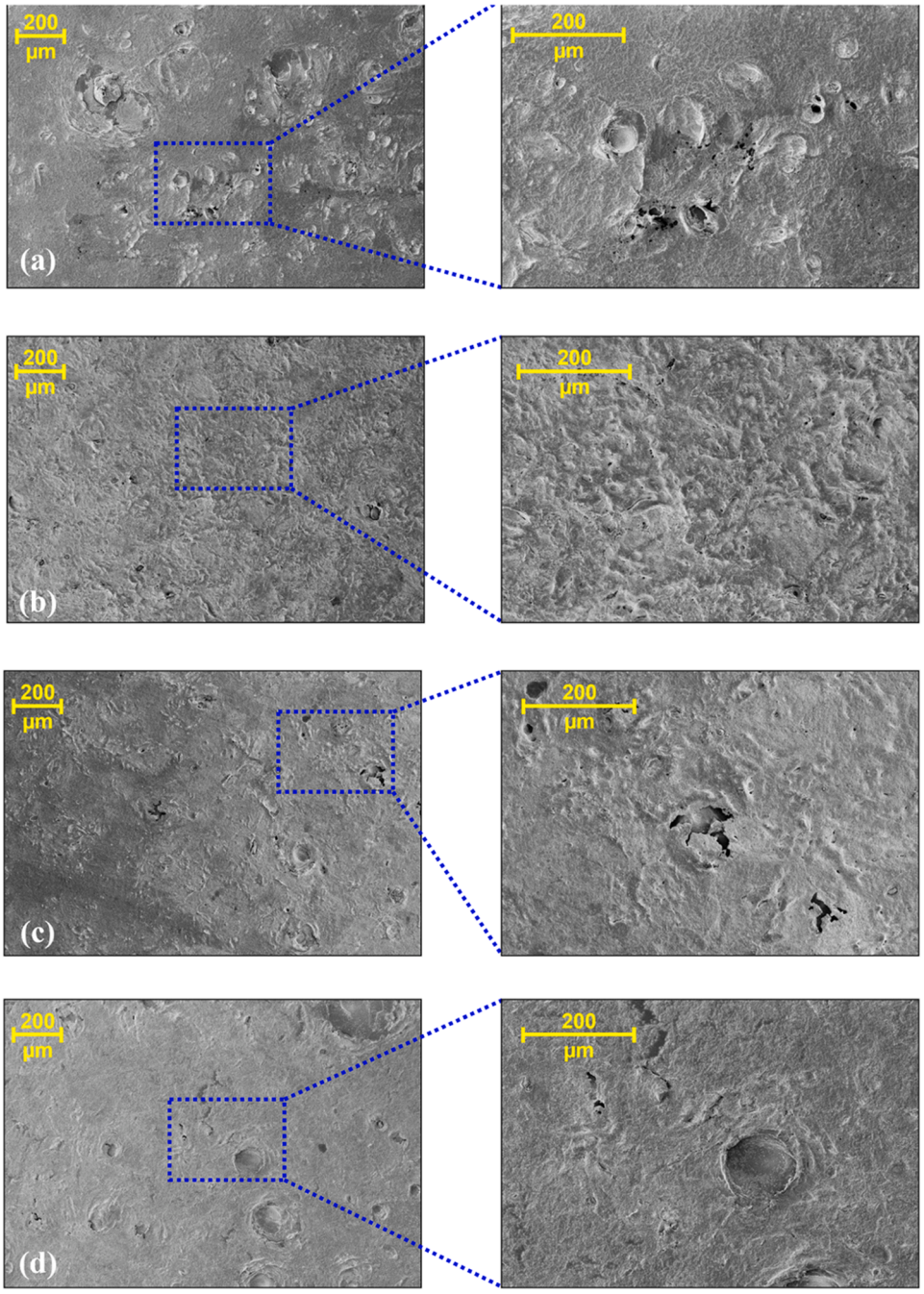

Fig. 7. The effect of process parameters on surface morphology and coverage a) pressure of air flow = 4 bar (SoD of 150 mm) b) pressure of air flow = 6 bar (SoD of 150 mm) c) SoD = 150 mm (pressure of 6 bar) d) SoD = 200 mm (pressure of 6 bar).

Table 4
Experimental surface roughness data measured on the as-received and sand blasted surfaces treated using an air pressure of 6 bar, SoD of 150 mm, and blasting time of 3 s.

	R_a (µm)	R_q (µm)	R_z (µm)	R_t (µm)	R_{max} (µm)
As-received specimen	0.02 ± 0.01	0.03 ± 0.01	0.12 ± 0.01	0.16 ± 0.03	0.16 ± 0.04
Sand blasted specimen	3.51 ± 0.14	4.51 ± 0.20	16.90 ± 0.54	23.68 ± 1.34	22.68 ± 0.86

4.1.2. Surface roughness

The results of surface roughness measurements on as-received and sand blasted specimens treated using a pressure of 6 bar, an SoD of 150 mm, and a blasting time of 3 s are listed in Table 4. The experimental roughness data confirm acceptable repeatability thanks to the optimized machine parameters utilized for stabilized sand blasting. Among the examined roughness parameters, R_a and R_q, which are respectively the average of absolute values and root mean square of the roughness, are global indexes. While the other parameters can be easily influenced by local features. This makes R_a and R_q the most characterizing roughness parameters. By analyzing these parameters, it is observed that the surface roughness is drastically increased after the application of sand

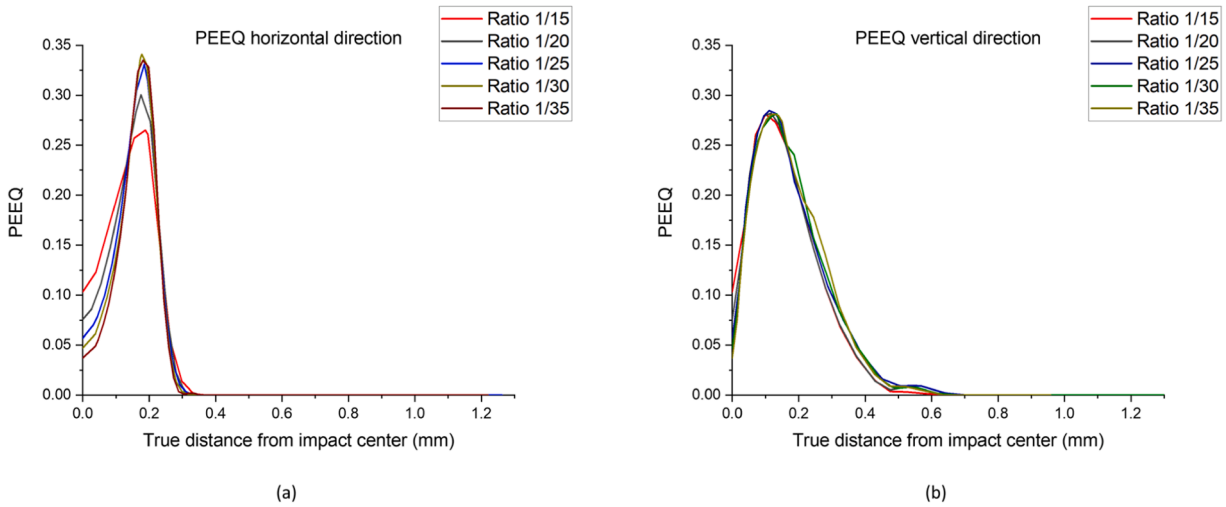

Fig. 8. Mesh convergence plots for PEEQ variation along (a) horizontal path and (b) vertical path, both starting from the center of a dimple induced by a single impact.

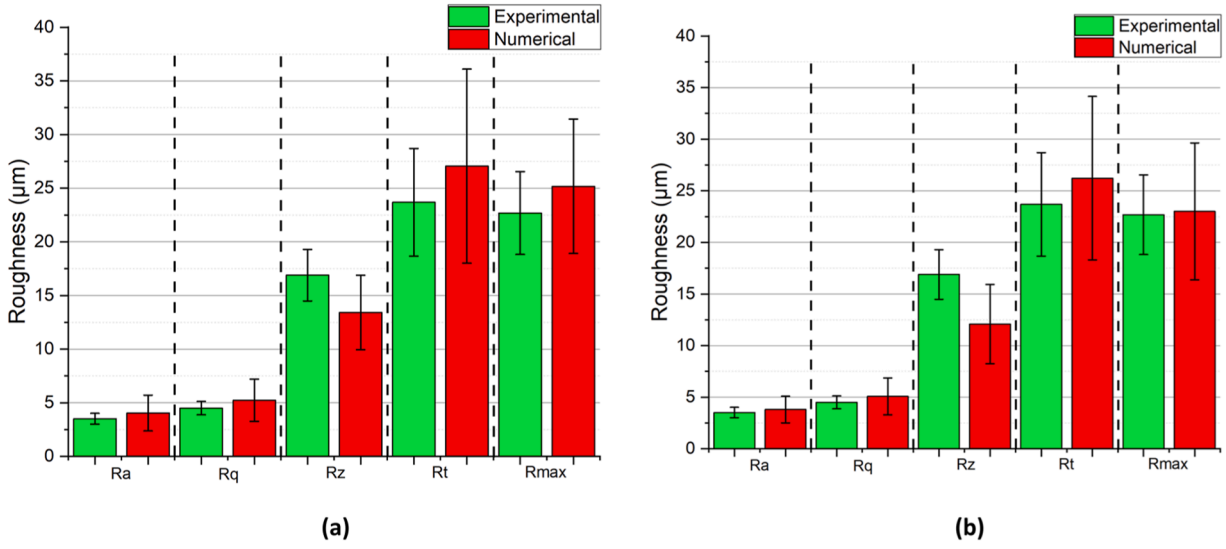

Fig. 9. Comparison of experimental and numerical roughness data for the simulation a) set-1 b) set-4.

blasting.

4.2. Numerical simulation results

4.2.1. Mesh convergence

The results of the mesh convergence study performed for the spherical shot (1 mm diameter) are presented in Fig. 8a and b in terms of the equivalent plastic strain (PEEQ). These results were extracted along two different paths starting from the dimple center: one along the dimple radius, and the other along the depth. The results indicated that the convergence was almost reached using an element size equal to 1/25th of the dimple diameter which is 0.022 mm.

4.2.2. Numerical assessment of surface roughness

In this section, the numerical surface roughness induced by sand blasting is presented and compared with the experimental data. The simulation introduced here relies on the random positioning of shots over the impact area using random generator functions. Thus, the model was run 6 different times to study the effect of varying sequences and randomized positions of shots on the final results. Fig. 9 shows the comparison of the average of experimental and numerical roughness parameters as well as the corresponding error values after full-coverage sand blasting for set-1 and set-4 as the representative cases, where the individual roughness parameters show a relatively good agreement. The error values in the numerical simulations were obtained using three randomly selected evaluation lines of 1.25 mm on the same impact area. The results of numerical simulations for set-1 to set-6 can be found in supplementary data in Table S1. Regarding the 6 trials, for the more global parameters such as R_a and R_q, the difference between the average values is mostly lower than 20% while for other local parameters, it mainly remains below 30%. Considering the range of the scatter and the complexities of modeling the sand blasting process regarding a wide range of media shape and size distribution, such differences are reasonable. It is noticed that regardless of the different random sequences for each set, the average results for the roughness parameters are in good agreement with the experimental data. This observation confirms that despite the assumed simplifications in particular for the media, the proposed model is capable of predicting successfully the

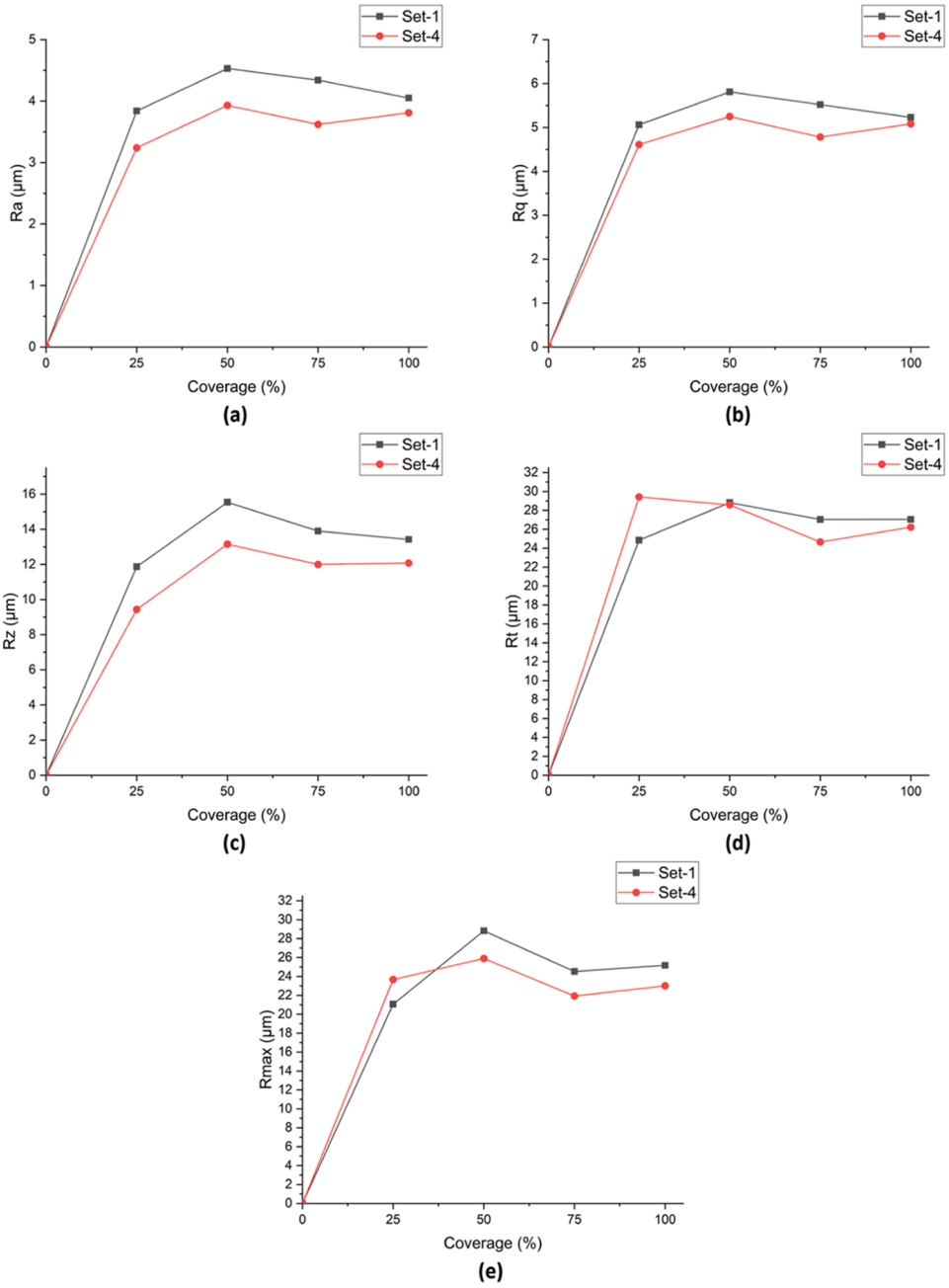

Fig. 10. Evolution of numerical surface roughness parameters with increasing coverage for set-1 and set-4 a) Ra b) Rq c) Rz d) Rt e) Rmax.

characteristics of the sand blasted surface.

Specifically, in the case of set-4, a very good match was noted between the numerical and experimental data (as shown in Fig. 9). To examine the reason behind this interesting trend, the shots' arrangement for this set was compared with that of set-1 as shown in Fig. 4a and d. It is clearly seen that set-1 has a more uniform shot distribution and the number of groups and sub-groups of the shots appear to have a more homogeneous dispersion. However, for set-4, a high portion of the impacts are made by cuboid shots. This higher number of cuboid shots provides a higher level of overlapping between the impacted areas. The results indicate that when the number of larger cuboid and tetrahedron shots is dominant, a better match can be obtained with experimental results in terms of surface roughness due to higher overlaying. In the case of simulating shot peening with spherical media using a similar numerical approach, it has been shown that different random shot sequences in terms of shot position result in very good repeatability of the numerical roughness parameters [40]. Based on these observations, it can be deduced that for the simulation of sand blasting, an improved algorithm should be used for the generation of shot arrangements to wisely steer the fraction of each shot sub-group in the generated sequence. This is considered to be a radical difference between the numerical modeling of the surface roughness induced by sand blasting and shot peening processes.

A further examination was done to investigate the evolution of the roughness parameters with increasing coverage levels below full coverage in numerical domain, as shown in Fig. 10. This can be helpful regarding the rate of changes in the roughness parameters with variations in the blasting time. The initial sharp increase in the roughness parameters below 25% coverage is conceivable due to the rapidly growing number of created indents over the not blasted surface. Then, the rate of change decreases till 50% coverage as more overlapping indents are induced. For most of the parameters, a peak value can be

identified at 50% coverage after which a decrease in the individual parameter is observed. It can be debated that with increasing sand blasting coverage, the already blasted surface is affected by the subsequent shot impacts such that the already induced peaks and valleys start decreasing beyond 50% coverage. This turns out to be a repeatable observation as a similar trend is observed for both set-1 and set-4. For all roughness parameters, a totally converging trend is noticed between two sets indicating that random sequences of different sets led to the separate evolutions of surface roughness but eventually a similar morphological state was obtained. This is a relatively analogous behavior of the roughness evolution in polymers compared to metallic materials [40].

5. Conclusion

A numerical model was developed to simulate the sand blasting process on polymeric substrates with the aim to reduce the experimental effort for tuning the process by serving as a tool to estimate the surface roughness as a function of process parameters.

The numerical model takes into account several parameters of the process including sand blasting machine characteristics (e.g., pressure and stand-off distance), shot and target material properties, and size and shape distribution of the irregular shot media. The model is also assisted with several scripts that define strategies for incorporating realistic assumptions for shot media morphology and size, evaluate shot impact velocity as a function of characteristics and interaction with the compressed air flow, induce several randomness factors and post-process the results to calculate surface roughness parameters.

Comparison of the numerical and experimental results demonstrated that the model can successfully estimate roughness parameters. The lowest discrepancy for Ra parameter was estimated to be around 8% that is well in line with the ranges predicted by shot peening simulations, keeping in mind that in shot peening the size and shape of the shots are normally estimated to be constant and thus the simulation has very less complexities compared to sand blasting.

As indicated by the better match obtained for one of the sets, a possible way to further enhance the agreement between numerical and experimental results can be to perform a more in-depth microscopy analysis of the media and verify the higher tendency of the shot media to be characterized with cuboid morphology. Thus, we envisage that an enhanced shot characterization possibly considering the dominancy of cuboid shots could improve the results.

Declaration of Competing Interest

The authors declare that they have no known competing financial interests or personal relationships that could have appeared to influence the work reported in this paper.

Data availability

Data will be made available on request.

Acknowledgment

E. O. and N. G. contributed equally to this work.

Supplementary materials

Supplementary material associated with this article can be found, in the online version, at doi:10.1016/j.finmec.2023.100208.

References

[1] J. Hasan, H.K. Webb, V.K. Truong, S. Pogodin, V.A. Baulin, G.S. Watson, J. A. Watson, R.J. Crawford, E.P. Ivanova, Selective bactericidal activity of nanopatterned superhydrophobic cicada Psaltoda claripennis wing surfaces, Appl. Microbiol. Biotechnol. 97 (2013) 9257–9262, https://doi.org/10.1007/s00253-012-4628-5.

[2] A. Rudawska, I. Danczak, M. Müller, P. Valasek, The effect of sandblasting on surface properties for adhesion, Int. J. Adhes. Adhes. 70 (2016) 176–190, https://doi.org/10.1016/j.ijadhadh.2016.06.010.

[3] N. Menga, R. Di Mundo, G. Carbone, Soft blasting of fluorinated polymers: the easy way to superhydrophobicity, Mater. Des. 121 (2017) 414–420, https://doi.org/10.1016/j.matdes.2017.02.074.

[4] R. Melentiev, C. Kang, G. Shen, F. Fang, Study on surface roughness generated by micro-blasting on Co-Cr-Mo bio-implant, Wear 428–429 (2019) 111–126, https://doi.org/10.1016/j.wear.2019.03.005.

[5] A. Raykowski, M. Hader, B. Maragno, J.K. Spelt, Blast cleaning of gas turbine components: deposit removal and substrate deformation, Wear 249 (2001) 126–131, https://doi.org/10.1016/S0043-1648(01)00518-X.

[6] R.K. Chintapalli, F.G. Marro, E. Jimenez-Pique, M. Anglada, Phase transformation and subsurface damage in 3Y-TZP after sandblasting, Dent. Mater. 29 (2013) 566–572, https://doi.org/10.1016/j.dental.2013.03.005.

[7] R.K. Chintapalli, A.M. Rodriguez, F.G. Marro, M. Anglada, Effect of sandblasting and residual stress on strength of zirconia for restorative dentistry applications, J. Mech. Behav. Biomed. Mater. 29 (2014) 126–137, https://doi.org/10.1016/j.jmbbm.2013.09.004.

[8] R.F.V. Rocha, L.C. Anami, T.M.B. Campos, R.M. de Melo, R.O. de A. e Souza, M. A. Bottino, Bonding of the polymer polyetheretherketone (PEEK) to human dentin: effect of surface treatments, Braz. Dent. J. 27 (2016) 693–699, https://doi.org/10.1590/0103-6440201600796.

[9] R. Ourahmoune, M. Salvia, T.G. Mathia, N. Mesrati, Surface morphology and wettability of sandblasted PEEK and its composites, Scanning 36 (2014) 64–75, https://doi.org/10.1002/sca.21089.

[10] D. Porrelli, M. Mardirossian, N. Crapisi, M. Urban, N.A. Ulian, L. Bevilacqua, G. Turco, M. Maglione, Polyetheretherketone and titanium surface treatments to modify roughness and wettability – improvement of bioactivity and antibacterial properties, J. Mater. Sci. Technol. 95 (2021) 213–224, https://doi.org/10.1016/j.jmst.2021.04.023.

[11] M. Lampin, R. Warocquier-Clérout, C. Legris, M. Degrange, M.F. Sigot-Luizard, Correlation between substratum roughness and wettability, cell adhesion, and cell migration, J. Biomed. Mater. Res. 36 (1997) 99–108, https://doi.org/10.1002/(SICI)1097-4636(199707)36:1<99::AID−JBM12>3.0.CO;2-E.

[12] M. Chen, H. Che, S. Yue, Exploring surface preparation for cold spraying on polymers, Surf. Coatings Technol. 450 (2022), 128993, https://doi.org/10.1016/j.surfcoat.2022.128993.

[13] X. Yu, X. Wei, X. Huang, L. Zhang, Study on the modeling method and influencing parameters of sandblasting process for blade grinding, Adv. Mater. Sci. Eng. 2022 (2022), 7905927, https://doi.org/10.1155/2022/7905927.

[14] H. Gerhardter, R. Prieler, S. Zausinger, C. Hochenauer, Investigating the advantages of Laval blasting nozzles in combination with injector-type sandblasters using efficient numerical methods, Surf. Coatings Technol. 445 (2022), 128699, https://doi.org/10.1016/j.surfcoat.2022.128699.

[15] H.Y. Miao, S. Larose, C. Perron, M. Lévesque, On the potential applications of a 3D random finite element model for the simulation of shot peening, Adv. Eng. Softw. 40 (2009) 1023–1038, https://doi.org/10.1016/j.advengsoft.2009.03.013.

[16] B. Bhuvaraghan, S.M. Srinivasan, B. Maffeo, Numerical simulation of Almen strip response due to random impacts with strain-rate effects, Int. J. Mech. Sci. 53 (2011) 417–424, https://doi.org/10.1016/j.ijmecsci.2011.03.004.

[17] G.I. Mylonas, G. Labeas, Numerical modelling of shot peening process and corresponding products: residual stress, surface roughness and cold work prediction, Surf. Coatings Technol. 205 (2011) 4480–4494, https://doi.org/10.1016/j.surfcoat.2011.03.080.

[18] P. Sanjurjo, C. Rodríguez, I. Peñuelas, T.E. García, F.J. Belzunce, Influence of the target material constitutive model on the numerical simulation of a shot peening process, Surf. Coatings Technol. 258 (2014) 822–831, https://doi.org/10.1016/j.surfcoat.2014.07.075.

[19] H. Chen, S. Wang, S. Lu, Y. Qiao, X. Wang, N. Fan, P. Guo, J. Niu, Simulation and experimental validation of residual stress and surface roughness of high manganese steel after shot peening, Procedia CIRP 71 (2018) 227–231, https://doi.org/10.1016/j.procir.2018.05.066.

[20] J. Wu, H. Liu, P. Wei, Q. Lin, S. Zhou, Effect of shot peening coverage on residual stress and surface roughness of 18CrNiMo7-6 steel, Int. J. Mech. Sci. 183 (2020), 105785, https://doi.org/10.1016/j.ijmecsci.2020.105785.

[21] S. Bagherifard, R. Ghelichi, M. Guagliano, Numerical and experimental analysis of surface roughness generated by shot peening, Appl. Surf. Sci. 258 (2012) 6831–6840, https://doi.org/10.1016/j.apsusc.2012.03.111.

[22] S. Bagherifard, R. Ghelichi, M. Guagliano, On the shot peening surface coverage and its assessment by means of finite element simulation: a critical review and some original developments, Appl. Surf. Sci. 259 (2012) 186–194, https://doi.org/10.1016/j.apsusc.2012.07.017.

[23] S. Bagherifard, R. Ghelichi, M. Guagliano, A numerical model of severe shot peening (SSP) to predict the generation of a nanostructured surface layer of material, Surf. Coatings Technol. 204 (2010) 4081–4090, https://doi.org/10.1016/j.surfcoat.2010.05.035.

[24] H. Khajehmirza, A.H. Astaraee, S. Monti, M. Guagliano, S. Bagherifard, A hybrid framework to estimate the surface state and fatigue performance of laser powder bed fusion materials after shot peening, Appl. Surf. Sci. 567 (2021), 150758, https://doi.org/10.1016/j.apsusc.2021.150758.

[25] J. Wu, H. Liu, P. Wei, C. Zhu, Q. Lin, Effect of shot peening coverage on hardness, residual stress and surface morphology of carburized rollers, Surf. Coatings Technol. 384 (2020), 125273, https://doi.org/10.1016/j.surfcoat.2019.125273.
[26] ISO 4288:1996 - Geometrical Product Specifications (GPS) — Surface texture: profile method — Rules and procedures for the assessment of surface texture, (1996) https://www.iso.org/standard/2096.html.
[27] Granta EduPack, (2021).
[28] A.K. Dwivedi, J. Bradley, D. Casem, Mechanical Response of Polycarbonate with Strength Model Fits, in: Army Research Laboratory, 2012.
[29] D. Kirk, Generation of Air-Blast Shot Velocity, (2007).
[30] H.Z. Li, J. Wang, J.M. Fan, Analysis and modelling of particle velocities in micro-abrasive air jet, Int. J. Mach. Tools Manuf. 49 (2009) 850–858, https://doi.org/10.1016/j.ijmachtools.2009.05.012.
[31] Z.Y. Liu, Y.B. Guo, C.Z. Huang, Kinematic modeling and deformation mechanics in shot peening of functional ceramics, Procedia Manuf. 5 (2016) 508–520, https://doi.org/10.1016/j.promfg.2016.08.042.
[32] D. Kirk, M.Y. Abyaneh, Theoretical basis of shot peening coverage control, in: Proceedings of the 5th International Conference on Shot Peening, 1993, pp. 183–190.
[33] D. Kirk, M.Y. Abyaneh, Theoretical basis of shot peening coverage control, Shot Peen. 9 (1995) 28–30.
[34] D. Kirk, M.Y. Abyaneh, Theoretical basis of shot peening coverage control, Shot Peen. 13 (1999) 5–7.
[35] D. Kirk, Shot peening, Aircr. Eng. Aerosp. Technol. (1999).
[36] M. Avrami, Kinetics of phase change. II transformation-time relations for random distribution of nuclei, J. Chem. Phys. 8 (1940) 212–224.
[37] M. Avrami, Granulation, phase change, and microstructure kinetics of phase change. III, J. Chem. Phys. 9 (1941) 177–184.
[38] M. Avrami, Kinetics of phase change. I general theory, J. Chem. Phys. 7 (1939) 1103–1112.
[39] S.E. Committee, Shot Peening Coverage Determination (2013). doi:10.4271/J2277_201304.
[40] A. Heydari Astaraee, S. Bagherifard, S. Monti, M. Guagliano, Evaluating the homogeneity of surface features induced by impact-based surface treatments, Materials (Basel) 14 (2021), https://doi.org/10.3390/ma14133476.